Chemical Kinetics of Hydrogen Atom Abstraction from Allylic Sites by $^3O_2$; Implications for Combustion Modelling and Simulation

Chong-Wen Zhou,*,† John. M. Simmie,† Kieran P. Somers,† C. Franklin Goldsmith,‡ and Henry J. Curran†

†*Combustion Chemistry Centre & School of Chemistry, National University of Ireland, Galway H91 TK33, Ireland*

‡*School of Engineering, Brown University, Providence, RI 02912, USA*

E-mail: chongwen.zhou@nuigalway.ie

Abstract

Hydrogn atom abstraction from allylic C–H bonds by molecular oxygen plays a very important role in determining the reactivity of fuel molecules having allylic hydrogen atom. Rate constants for hydrogen atom abstraction by molecular oxygen from molecules with allylic sites have been calculated. A series of molecules with primary, secondary, tertiary and super secondary allylic hydrogen atoms of alkene, furan and alkyl-benzene families are taken into consideration. Those molecules include propene, 2-butene, isobutene, 2-methylfuran and toluene containing the primary allylic hydrogen atom; 1-butene, 1-pentene, 2-ethylfuran, ethylbenzene and *n*-propylbenzene containing the secondary allylic hydrogen atom; 3-methyl-1-butene, 2-isopropylfuran and isopropylbenzene containing tertiary allylic hydrogen atom; and 1-4-pentadiene containing super allylic secondary. The M06-2X/6-311++G(d,p) level of theory was used to optimize the geometries of all of the reactants, transition states, products and also the hinder rotation treatments for lower frequency modes. The G4 level of theory was used to calculate the electronic single point energies for those species to determine the barriers at 0 K to reaction. Conventional transition state theory with Eckart tunnelling corrections was used to calculate the rate constants. The comparison between our calculated rate constants with the available experimental results from the literature shows good agreement for the reactions of propene and isobutene with molecular oxygen. The rate constant for toluene with O_2 is about an order magnitude slower than that experimentally derived from a comprehensive model proposed by Oehlschlaeger and co-authors. The results clearly indicate the need for a more detailed investigation of the combustion kinetics of toluene oxidation and its key pyrolysis and oxidation intermediates. Despite this, our computed barriers and rate constants retain an important internal consistency. Rate constants calculated in this work have also been used in predicting the reactivity of the target fuels of 1-butene, 2-butene, isobutene, 2-methyl furan, 2,5-dimethyl furan and toluene, and the results show that the ignition delay times for those fuels have been increased by a factor of 1.5 to 3. This work provides a first systematic study of one of the key initiation reaction for compounds

containing allylic hydrogen atoms.

Introduction

There is currently much interest in so-called 'lower temperature' combustion which aims to reduce emissions without leading to poor engine efficiency and higher fuel consumption. At these lower temperatures the reactions of molecular oxygen, and those of associated radicals such as hydroperoxyl, are progressively more important. Moreover, in the comprehensive chemical model development for propene,[1] isobutene,[2] 1-butene,[3] 2-butene,[4] 2-methylfuran,[5] 2,5-dimethylfuran[6] and toluene,[7] it was shown that hydrogen atom abstraction by molecular oxygen of allylic hydrogen atoms plays an important and interesting role in determining the reactivity of these fuels. Taking the butene isomers as examples, it is shown that the reaction $RH + {}^3O_2 \rightarrow \dot{R} + H\dot{O}_2$ is endothermic and at lower temperatures (<900 K) this reaction is favored in the reverse direction which consumes two radical, one allylic-type and a hydroperoxyl radical to form two stable molecules, inhibiting the reactivity,[1;2] while at higher temperatures (>900 K), this reaction occurs in the forward direction and promotes reactivity,[1.2] Under fuel-rich conditions at high temperatures (>1200 K), this is the reaction that most promotes fuel reactivity. However, there are very few measurements or calculations available in the open literature[9] for the rates of reaction of families of compounds with ground-state triplet dioxygen $O_2({}^3\Sigma_g^-)$, particularly those which involve hydrogen-atom abstraction, as opposed to studies with singlet $O_2({}^1\Delta_g)$. For similar reaction processes, the rate constants used in models[1,2,4–7] can be as much as one order of magnitude different and a systematic investigation of this type of reactions are crucially important to provide accurate reactivity predictions for these fuels under engine condition.

Park et al.[8] have investigated the singlet and triplet potential energy surfaces for the reaction of O_2 with C_2H_4 at the MRMP2/aug-cc-pVDZ//CASSCF level of theory. They

proposed that the addition barrier to form $C_2H_4O_2$ is 141.4 kJ mol^{-1} on the triplet potential energy surface and the subsequent decomposition reaction of $C_2H_4O_2$ needs to overcome a barrier of at least 87.8 kJ mol^{-1} which means for the addition reaction channels, the reaction needs to overcome a barrier height of 229.2 kJ mol^{-1} which is not competitive as the barriers of allylic hydrogen abstraction by molecular oxygen are around 167.3 kcal mol^{-1}. In this work, we just focus on the hydrogen abstraction channels and ignored the triplet O_2 addition reaction channels which are not important in this context.

In *this work* we explore the chemical kinetic consequences of structural variants of allylic H-atom sites from which $O_2(^3\Sigma_g^-)$ abstracts a hydrogen atom: X—C**H**$_3$, X—C**H**$_2$CH$_3$, X—C**H**$_2$C$_2$H$_5$ and X—C**H**(CH$_3$)$_2$ where X is allyl, 2-furyl or phenyl; together with the alkylated propenes, cis- and trans-but-2-enes and iso-butene C**H**$_3$—CH=CH—C**H**$_3$, CH$_2$=C(C**H**$_3$)$_2$, penta-1,4-diene which contains a super-allylic site CH$_2$=CH—C**H**$_2$—CH=CH$_2$ and hexa-1,5-diene, CH$_2$=CH—C**H**$_2$—C**H**$_2$—CH=CH$_2$, which does not.

For the simplest alkene with allylic site, propene, the earliest experimental work was from the Walker group[10] who studied the slow reaction in a batch reactor. Their results were later confirmed by Barbe et al.[11] and adopted by a comprehensive review.[12] Similar experiments by the Walker group showed that iso-butene was four times more reactive than propene over the temperature range of 673 – 793 K.[13]

Shock wave experiments in which the formation of benzyl radicals was followed by UV-absorption at 266 nm by two groups[14,15] at temperatures in the range of 1100 – 1400 K gave reasonable concordant results for H-atom abstraction by molecular oxygen from toluene.

Computational methodology

Geometry optimizations and frequency determinations were carried out with the functionals and basis sets M06-2X/6-311++G(d,p).[29] The recommended vibrational scale factor of 0.983 for this method was used.[30] Relaxed potential energy scans were employed to account

for the presence of hindered rotors. The dihedral scans over 360° at 10° intervals were fitted to a Fourier-series as were the moments of inertia for asymmetric scans but for symmetric scans such as those of methyl groups only the barrier to rotation and harmonic frequencies were required to count the hindered rotor energy levels. A mid-level composite method, G4, which is contained within the Gaussian-09 application was used to compute the zero-point electronic energies of all reactants, complexes, transition states and products.[16,17] Additional computations were carried out at QCISD(T) in the complete basis set limit and also with the W1 variant W1BD[18] in order to check the barrier height for the key reaction: $C_3H_6 + {}^3O_2$. Diagnostic tests indicate that these single-reference methods provide an adequate treatment of the electronic structure.[19,20] Typically T1 diagnostics in this study are lower than 0.036 with a very few up to 0.040 for the super allylic site. For transition states, which exhibited just one imaginary frequency, additional intrinsic reaction coordinate calculations were required to establish the connection between reactants and products.[21,22] Typically C····H bond distances of 1.434 Å, O····H bondlengths of 1.146 Å and CHO angles of 171° are found, as were both pre- and post-reaction complexes. Conventional transition state theory with Eckart tunnelling corrections taken into consideration was used to calculate the rate constants. Thermochemical and kinetic calculations were performed with Thermo/Multiwell[23] and Variflex codes.[24]

In addition to the G4 calculations, two additional methods were considered in the propene reaction. In the first method, the geometry optimization and normal-mode analysis for the stationary points on the potential energy surface were performed using a different density functional, M11/MG3S.[25] Single-point calculations were performed using explicitly correlated coupled cluster, CCSD(T)-F12a/cc-pVTZf12.[26] Additionally, benchmark calculations were performed using the methods in Goldsmith et al[27] with only a brief summary is provided here. Geometry optimization and normal mode analysis were performed at UCCSD(T)/cc-pVTZ level of theory. The following sequence of corrections were then applied: basis-set extrapolation using aug-cc-pVQZ and aug-cc-pV5Z basis sets; core valence correlations were

estimated based upon the difference between UCCSD(T)/aug-cc-pcV∞Z energies in which the core electrons are frozen and unfrozen, with basis set extrapolation obtained from TZ and QZ basis sets; relativistic effects from the difference in the configuration interaction energy within and without the Douglas-Kroll one-electron integrals. The correction for higher-order excitations using perturbative quadruples, UCCSDT(Q)/cc-pVDZ, was computationally too demanding for this application. For both the F12//M11 and the benchmark calculations, torsional modes were treated as 1D hindered internal rotors, with rotational potentials calculated via a constrained optimization in 10° increments using M11/MG3S. The torsional partition function was solved from the corresponding 1D Schrödinger equation. These calculations were performed using the *ab initio* rate theory package PAPR from Argonne National Laboratory.[28]

Results

A summary of the quantum calculations are presented in Table 2 from which it can be seen that the zero-point corrected electronic energy reaction barriers decrease along the series primary, secondary and tertiary hydrogens in a consistent manner for X = vinyl, 2-furyl and phenyl. The vinyl and 2-furyl series are particularly uniform, 167 $\rightarrow$ 156 $\rightarrow$ 146 kJ mol^{-1}, with the phenyl derivatives showing a lesser decrease of 167 $\rightarrow$ 160 $\rightarrow$ 156 kJ mol^{-1} along the sequence $-\mathrm{C}\mathbf{H}_3 \rightarrow -\mathrm{C}\mathbf{H}_2\mathrm{CH}_3 \rightarrow -\mathrm{C}\mathbf{H}(\mathrm{CH}_3)_2$. The most dramatic lowering in barrier height is shown by the 'super-allylic' H-atoms in 1,4-pentadiene which are even more reactive than tertiary sites. By way of contrast the secondary sites in the closely related hexa-1,5-diene are 'normal'.

Monomethylation of propene can be accomplished at the 2- and 1-positions and this results in a slight lowering of the barrier from 167 to $\sim$ 160 kJ mol^{-1}. Dimethylation to yield 2-methyl-but-2-ene results in a compound with three different abstractable primary H-atoms whose barriers are $\sim$ 152 kJ mol^{-1} whilst complete methylation to give 2,3-dimethyl-

2-butene or tetramethylethylene lowers the barrier yet further to 143 kJ mol^{-1}. The general decrease in barrier heights from propene through 2,3-dimethyl-but-2-ene is paralleled by the decrease in the C—H bond dissociation energies.[31]

For the reactions involved in this work, a stepwise mechanism involving the formation of a reactant complex (RC) in the entrance channel and product complex (PC) in the exit channel has been determined. Taking the reaction between propene and $+^3O_2$ for example, the reaction pathway can be written as $C_3H_6 + {}^3O_2 \rightarrow RC \overset{TS}{\rightarrow} PC \rightarrow C_3H_5 + HO_2$. The Van der Waals interaction exists in both RC and PC can lower the energies by 6.7 and 50 kJ mol^{-1} respectively. Heat of reactions at 0 K are also shown in Table 2 from which it can be seen that all of these reactions are endothermic. Product complexes play important roles for the reactions whose energy of the products look higher than the transition states.

Discussion

As summarized earlier there are a few experiments and theoretical calculations against which our computed values can be validated.

Propene

Stothard and Walker[10] carried out batch reactor studies of the slow reaction between propene and oxygen to yield allyl and hydroperoxyl radicals, at four temperatures between 673 and 793 K and deduced $A = 10^{12.29\pm0.41}$ cm^3 mol^{-1} s^{-1} and $E_a = 163.5 \pm 6$ kJ mol^{-1}. In a later work they showed that the intermediate formed from allyl radical recombination, namely hexa-1,5-diene, reacted some 1,000 times faster than propene itself.[32] This complication might indicate that their original rate constant is over-estimated. However, the barrier height for H-atom abstraction by $^3O_2$ from the secondary sites in the diene is not significantly lower than for the other species being considered here and is in fact identical to that for 1-pentene.

Table 1: Barrier heights and heat of reactions at G4(0 K) in kJ mol^{-1}, imaginary frequencies / cm^{-1}.

Reactant	$E^{\dagger}$	$i\nu$	Δ_rH
Primary			
CH_2=CHC**H**$_3$	166.6	1747	157.3
CH_2=C(C**H**$_3$)$_2$	162.8	1689	162.0
C**H**$_3$CH=CH(C**H**$_3$) cis	156.6	1831	154.7
C**H**$_3$CH=CH(C**H**$_3$) trans	158.9	1778	154.7
$(CH_3)_2$C=CHC**H**$_3$	148.8	1799	148.8
CH_3CH=C(C**H**$_3$)$_2$ cis	153.0	1756	156.3
CH_3CH=C(C**H**$_3$)$_2$ trans	154.7	1817	155.8
(C**H**$_3$)$_2$C=C(C**H**$_3$)$_2$	142.7	1832	146.7
2-methylfuran	167.0	2010	155.4
toluene	167.0	1385	169.5
Secondary			
CH_2=CHC**H**$_2$$CH_3$	155.8	1878	143.1
CH_2=CHC**H**$_2$$CH_2CH_3$	153.8	1877	143.8
CH_2=CHC**H**$_2$C**H**$_2$CH=CH_2	153.2	1842	143.9
2-ethylfuran	155.8	1994	144.8
ethylbenzene	160.0	1752	158.4
n-propylbenzene	158.5	1728	161.5
Tertiary			
CH_2=CHC**H**$(CH_3)_2$	146.3	1900	133.4
2-isopropylfuran	145.0	1994	135.3
isopropylbenzene	155.9	1794	154.6
'Super' Secondary			
CH_2=CHC**H**$_2$CH=CH_2	139.5	2037	116.2

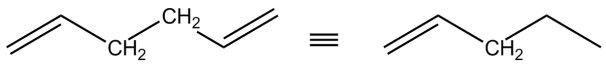

Thus, a rate constant enhancement by a factor of 1,000 is most unlikely. Of course the experimental result is probably overestimated given the employment of batch reactors and the low temperatures used in that study — factors which enhance the probability of surface-catalysed reactions.

In theoretical calculations of the reverse process Goldsmith et al.[33] computed, inter alia, for $\dot{C}_3H_5 + H\dot{O}_2 \xrightarrow{k_{1a}} C_3H_6 + {}^3O_2$ a rate constant of $k_{1a} = (9.3 \pm 0.1) \times 10^{-15}\, T^{2.7}\, \exp\{(490 \pm 10)/T\}$ cm^3 molecule^{-1} s^{-1}. Their work was carried out at QCISD(T)/CBS//B3LYP/MG3S levels of theory; in conjunction with their thermochemistry they computed a value for the reverse reaction and found that it was a factor of 5 too slow in comparison to the Stothard and Walker measurements. They modified their calculations by manipulating the barrier height of 171 kJ mol^{-1} but even so struggled to match the measurements and consequently suggested that the experiments might be as much as a factor of 30 too fast.

Our G4 result of 166.6 kJ mol^{-1}, Table 2, is therefore not too wide of the mark. This is reinforced by Brueckner coupled cluster doubles with a triples contribution BD(T), or W1BD, calculations which indicate a zero-point corrected electronic energy barrier height of 168.6 kJ mol^{-1}. Reasonable agreement with experiment is obtained, Fig. 1, with our calculations within 50% at the lowest temperature, improving to within 20% at the highest temperature. The barrier height for this reaction has also been calculated at UCCSD(T)-F12a/cc-pVTZf12//M11/MG3s and UCCSD(T)/CBS//UCCSD(T)/cc-pVTZ levels of theory separately and the comparison of results from these three methods are shown in Table. 2. The electronic energy barrier obtained at G4 level of thoery is 3.1 kJ mol^{-1} higher than that from the benchmark method obtained at UCCSD(T)/aug-cc-pV∞Z/UCCSD(T)/cc-pVTZ level of thoery which is within the uncertainty of the electronic energy calculations. While on the opposite, the barrier height obtained at UCCSD(T)-F12a/cc-pVTZf12//M11/MG3S level of theory is 3.7 kJ mol^{-1} lower than that from the benchmark method which is also

still within the electronic energy calculation uncertainty. The frequencies and hindered rotor potential for these three methods are also treated at different level of theories, together with the electronic energy barrier difference, their influce to the final rate constants are shown in Fig. 1.

Table 2: Comparison of methods for $CH_2{=}CHCH_3$. Barrier heights in kJ mol^{-1}, imaginary frequencies / cm^{-1}.

method	$E^\dagger$	$i\nu$
G4	166.6	1747
UCCSD(T)-F12a/cc-pVTZf12//M11/MG3S	159.8	2139
UCCSD(T)/aug-cc-pV∞Z//UCCSD(T)/cc-pVTZ	163.5	2180

Isobutene

Experiments on isobutene $+{}^3O_2$ by Ingham et al.[13] over a narrow temperature range of 689 – 818 K yielded $k = 4.79 \times 10^{12}$ exp$(-19,360/T)$ cm^3 mol^{-1} s^{-1}. Our own rate constant is in reasonable agreement with CBS-q theoretical calculations by Chen and Bozzelli[34] of $k = 1.86 \times 10^9\, T^{1.30}$ exp$(-20,570/T)$ cm^3 mol^{-1} s^{-1} and is lower than experiment, Fig. 2, but in tolerable agreement, deviating from experimental results by a factor of 2.5 to 1.6 in the temperature range from 698 K to 818 K.

Toluene

H-atom abstraction from toluene by molecular oxygen has been studied in shock-heated gases from 1117 to 1366 K and total pressures of $\approx$ 1 bar.[15] These measurements are broadly similar to earlier shock tube results by Eng and co-workers who employed not dissimilar conditions.[14] The rate constant of $2.18 \times 10^7\, T^{2.5}$ exp$(-23,170/T)$ cm^3 mol^{-1} s^{-1} emerged from a consideration of a number of competing reactions and their assumed rate constants, from an upper limit for k of < 30 cm^3 mol^{-1} s^{-1} at 773 K by the Walker group[13] and from constraining the pre-exponential temperature dependence to $T^{2.5}$. As previously our

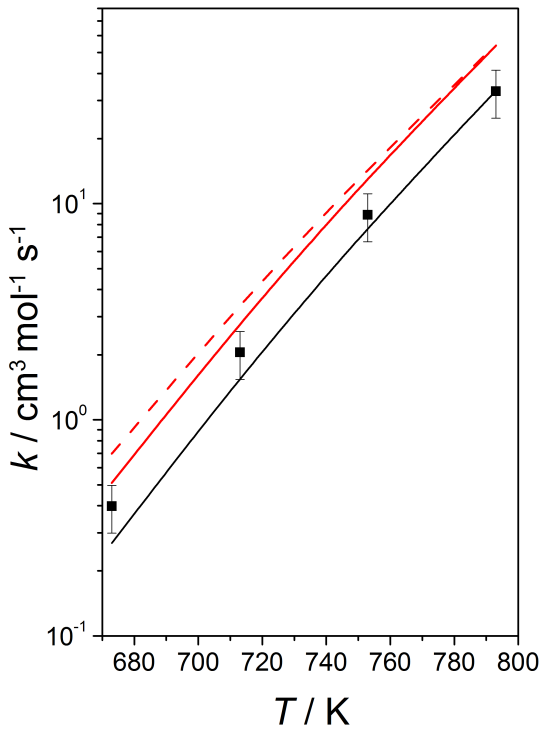

Figure 1: $C_3H_6 + {}^3O_2 \rightarrow \dot{C}_3H_5 + H\dot{O}_2$; ⊡ experiment[10] with added 25% error bars — G4//M062x/6-311++G(d,p), – – UCCSD(T)-F12a/cc-pVTZf12//M11/MG3S, — UCCSD(T)/aug-cc-pV∞Z//UCCSD(T)/cc-pVTZ.

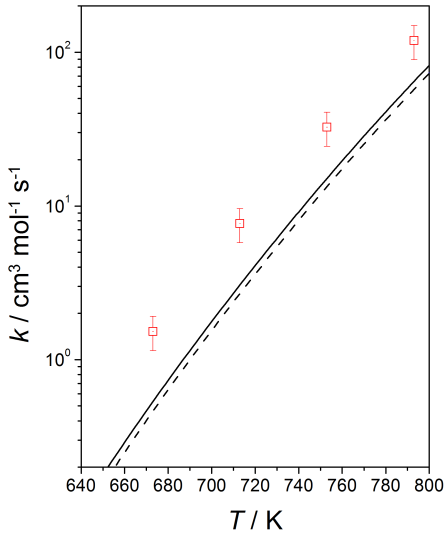

Figure 2: $CH_2{=}C(CH_3)_2 + {}^3O_2 \rightarrow CH_2{=}C(CH_3)\dot{C}H_2 + H\dot{O}_2$; ⊡ experiment[13] with added 25% error bars, – – Chen and Bozzelli,[34] — *this work*.

computed rate constants are lower than the experimental values, Fig. 3, but now by an order of magnitude margin.

In order to rationalise the observed discrepancies between our computed rate constant for the toluene system and that derived by Oehlschlaeger *et al.*,[15] we revisit their original experimental and modelling results. The extraction of a rate constant for the reaction of interest *via* shock heating of a toluene/oxygen/helium/argon mixture at a specific temperature and pressure is not straightforward. The measured absorption must be converted to benzyl mole fractions and for this the temperature-dependent molar absorptivity of both toluene and benzyl radical must be known at a wavelength of 266 nm. In the case of Oehlschlaeger's experiments, this was non-problematic, as previous studies[36,37] had provided this information to a high level of accuracy. However, other aromatics (benzoxyl radical, benzaldehyde, benzylperoxyl, bibenzyl, benzene, phenyl) are expected to be formed in some quantities from subsequent reactions, although their contributions to the measured absorption were not considered at the time and it is unknown how inclusion of contributions of these species to the measured absorption would influence the interpretation of their results.

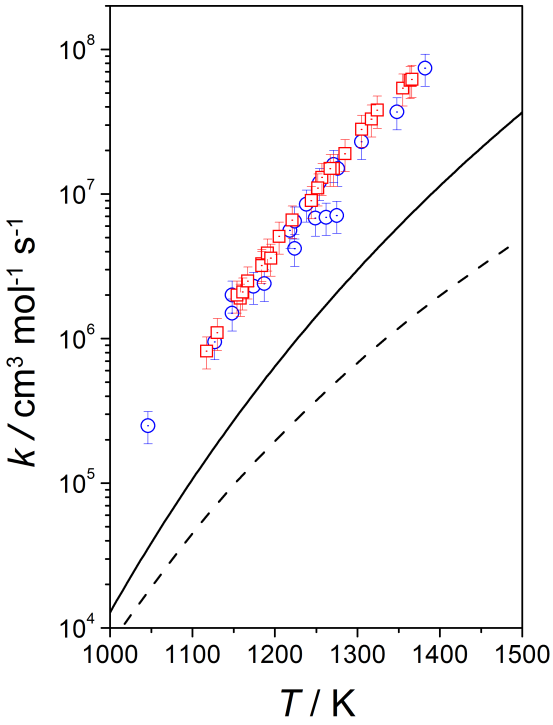

Figure 3: $C_6H_5CH_3 + {}^3O_2 \rightarrow C_6H_5\dot{C}H_2 + H\dot{O}_2$; experiment: ⊡,[15] ⊙[14] with added 25% error bars, – –,[35] — *this work*.

The extraction of a rate constant from their data also requires a comprehensive detailed chemical kinetic mechanism which introduces further uncertainty unless the model is well-constrained. Most available toluene models[38–41] currently employ the Oelschlaeger *et al.* rate constant apart from the earlier work by Bounaceur et al. who used a much lower value,[35] and test simulations show that the mechanisms which utilise the Oehlschlaeger *et al.* rate constant are capable of replicating thir reported benzyl yields. Here, we employ a recently optimised toluene combustion mechanism from Zhang *et al.*[7] for a secondary interpration of the experimental results. It is worth noting that the development of this model was motivated by discrepancies observed in the predictions of ignition delay times from available toluene kinetic models, and even a decade after Oehlschlaeger and co-workers' study, one still cannot approach the modelling of their experiments with the assumption that there is a *de facto* model in the literature capable of describing the combustion of toluene.

Table 3: Mixture mole percentages and reflected shock temperatures and pressures used in detailed chemical modelling of Oehlschlaeger *et al.*[15] experiements.

Toluene	O_2	He	Ar	T / K	p / bar
0.1	10	10	79.9	1117–1366	1.53–1.85
0.2	10	10	79.8	1154–1267	1.67–1.85

Here we simulate their shock tube as as a constant volume homogeneous batch reactor using the Aurora package of Chemkin-PRO,[42] under the reflected shock conditions reported in Table 3. For brevity, only the results for the mixtures containing 0.1 mol % of toluene will be discussed in the main text, with the results for the 0.2 mol % toluene mixtures provided in the Supporting Information. The resulting experimental and theoretical benzyl radical profiles are reported in Figure 4, where predictions of the original Oehlschlaeger *et al.* data are compared with predictions from the same mechanism where the rate constant for $C_6H_5CH_3 + {}^3O_2 \rightarrow C_6H_5\dot{C}H_2 + H\dot{O}_2$ has been updated with our newly derived value. The predictions of the original mechanism of Oehlschlaeger *et al.*[15] are in excellent agreement with the data, whilst the benzyl mole fractions are found to be grossly under-predicted upon

adoption of our new rate constant, in-line with the order of magnitude decrease in the rate constant for this important initiation reaction.

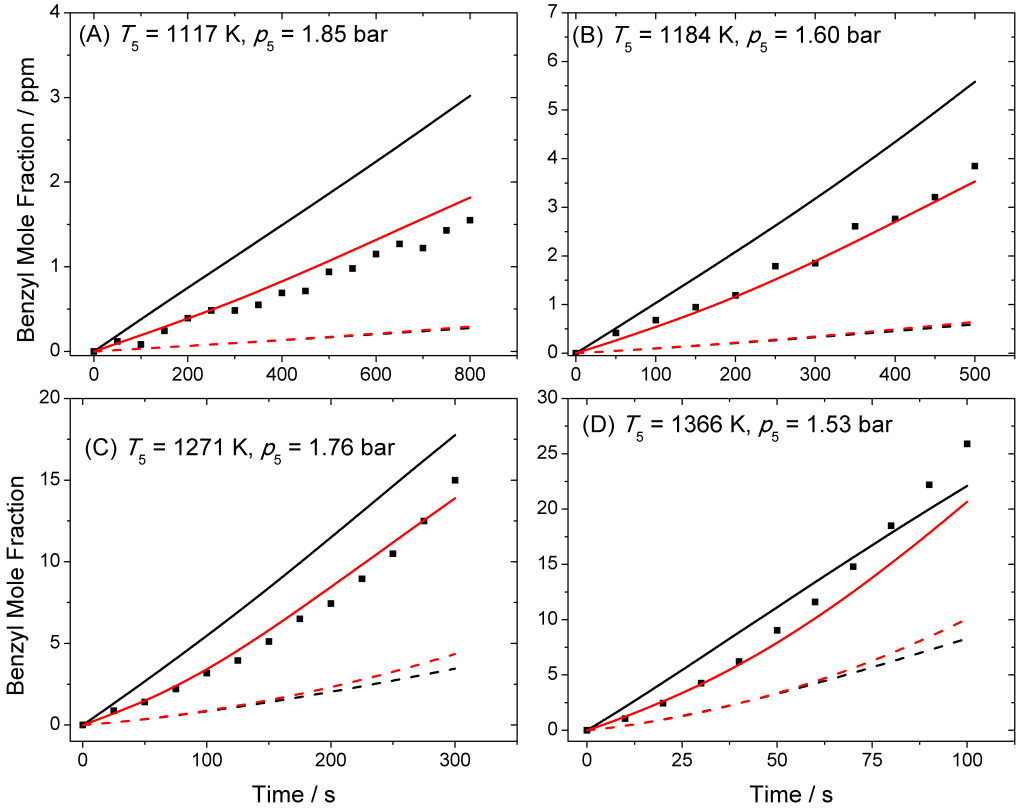

Figure 4: Experimental[15] (symbols) and predicted (lines) benzyl mole fractions for 0.1% toluene/O_2/He/Ar mixtures. Modelling results: Oehlschlaeger *et al.*[15] (—), Zhang *et al.*[7] (—). Dashed lines correspond to the same mechanisms with the rate constant for $C_6H_5CH_3 + {}^3O_2 \rightarrow C_6H_5\dot{C}H_2 + H\dot{O}_2$ adopted from *this work*.

Figure 4 also shows the predictions from the Zhang *et al.*[7] model which employs a rate constant for $C_6H_5CH_3 + {}^3O_2 \rightarrow C_6H_5\dot{C}H_2 + H\dot{O}_2$ based on the derived rate constant of Oehlschlaeger *et al.*,[15] with a factor of two increase to their originally recommended pre-exponential factor, this alteration being made to give a better account of ignition delay times measured in shock tubes and rapid compression machines for toluene/dimethyl ether mixtures. This adjustment leads to an over-prediction of the benzyl yields, and adoption of our updated rate constant into this mechanism again leads to an under-prediction of the benzyl mole fractions. So, despite employing a much more current and detailed chemical mechanism than that one by Oehlschlaeger *et al.* the predictions appear to be invariant

to the underlying chemistry and one must conclude as Oehlschlaeger *et al.* did, that the theoretically derived benzyl radical yields are most sensitive to the rate constant for the reaction of toluene with O_2. Therefore, one cannot resolve the current discrepancies without making order-of-magnitude variations to our theoretical result, without drastic revisions to available kinetic models, or without a detailed re-interpretation of the experimentally measured absorption profiles which might account for contributions to absorption from secondary species.

Whilst the uncertainties in our computed rate constants are probably of the order of a factor of 2–3 at any given temperature, the application of a consistent method to each of the alkenes studied leads to an internally consistent set of results—Figure 1 shows that our theoretical methods are quite capable of predicting the absolute rate constant for the reaction $C_3H_6 + {}^3O_2 \rightarrow \dot{C}_3H_5 + H\dot{O}_2$ as measured by Stothard and Walker[10] and in turn Figure 5 shows that the rate constants for abstraction of a hydrogen atom from propene, iso-butene and toluene are within a factor of $\approx$ 4–1.5 of each other in the range of 500–2000 K. Further to this, in the temperature range 600–800 K our computations give a very reasonable account of the relative rate constants as measured by Stothard and Walker[10] and Ingham et al.,[13] being within a factor of 3 of the experimentally derived values. At the higher temperature ranges where Oehlschlaeger *et al.* derived their rate constant, significant alterations to our computed entropies and enthalpies of activation would be required to fit their data which would diminish the predictions of the rate constants measured by others.[10] A systematic experimental study of the reactions of propene, iso-butene and toluene with O_2 would be of great utility in reconciling the current experiment and theory with a consistent detailed chemical kinetic model[1,2,4,7] now available in the literature to interpret such measurements.

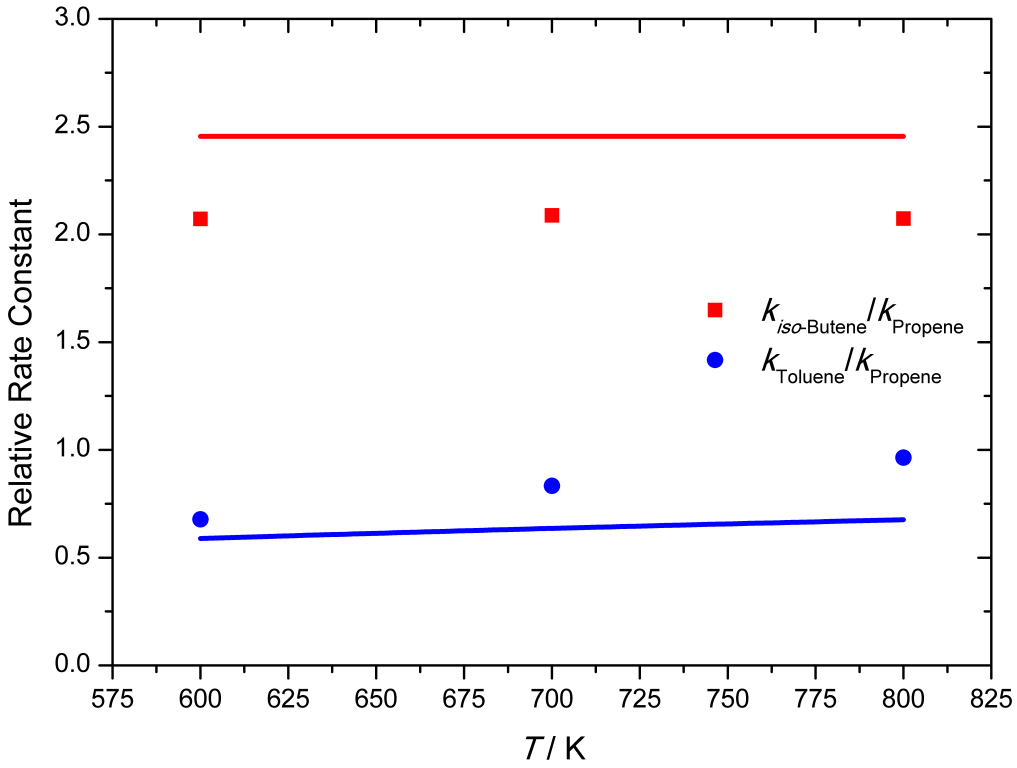

Figure 5: Relative rate constants for abstraction of a hydrogen atom by O_2 from propene, iso-butene and toluene. Symbols are the relative rate constants as computed based on the experimental results of Stothard and Walker[10] and Ingham et al.,[13] lines are based on computations of *this work*.

Singlet O_2 reactions

The suggestion has been made[43] that excited electronic states of O_2 may play a role in the results of the shock tube experiments.[15] As regards thermodynamics there is no appreciable difference between the properties, [S, C_P and $f(H)$] of the ground state X $^3\Sigma_g^-$ and that of the first excited state, a $^1\Delta_g$, which lies 390 kJ/mol above the ground state for temperatures less than 2000 K.[44] Even at the highest temperature the differences are less than 2% for the most affected, C_P, and even less for the entropy and the enthalpy function. As regards the kinetic aspects the equilibrium constant, $K = [\mathrm{a}\ ^1\Delta_g]/[\mathrm{X}\ ^3\Sigma_g^-]$, lies heavily on the ground state side with $K = 0.349\ \exp(-11,357/T)$. Below 900 K there is less than 1 ppm of $a^1\Delta_g$ in equilibrium with the ground state whilst at the highest temperature of the shock wave experiments of 1366 K this increases to 86 ppm. Hence quite considerable rate enhancements of the reaction:

$$\mathrm{C_6H_5CH_3 + O_2(a\ ^1\Delta_g) \rightarrow C_6H_5\dot{C}H_2 + H\dot{O}_2}$$

over that for:

$$\mathrm{C_6H_5CH_3 + O_2(X\ ^3\Sigma_g^-) \rightarrow C_6H_5\dot{C}H_2 + H\dot{O}_2}$$

would be required for the measurements to be strongly influenced by the excited O_2 state.

Rate constants for the reaction between singlet O_2 and propene, isobutene which are well-known ene Schenck reaction[45] and toluene have also been calculated in this work. Transition states for those fuel molecules with singlet O_2 reactions are quite different from the hydrogen atom abstraction reactions from these same molecules by triplet O_2. Taking the transition state for the reaction between singlet O_2 and propene shown in Fig. 6a as an example, O1 will abstract the allylic hydrogen atom H5 and O2 adds to the terminal vinylic carbon atom of C1. These two reaction processes happen simultaneously and a stable CH_2CHCH_2OOH molecule, 2-propenyl hydroperoxide, is formed with heat of formation of -51.9 kJ mol^{-1} [46] shown in Fig. 6c. The energy barrier for this reaction is 29.6 kJ mol^{-1} which is 137.0 kJ mol^{-1} *lower* than the triplet O_2 abstraction reaction barrier. The same reaction pathways

with much lower reaction barrier of 22.6 kJ mol^{-1} have also been found for the singlet O_2 reaction with isobutene, Fig. 6b and Fig. 6d. We should also bear in mind that singlet O_2 lies 390 kJ mol $^{-1}$ higher than the triplet O_2. Even though, reaction with singlet O_2 has much lower barrier heights, it is still not favored.

With toluene there is much more complexity where the hydrogen atom abstraction and singlet O_2 addition reactions can be seperated through different transition states of Figs. 7a, 7b and 7c with barriers of 65.8, 30.6 and 38.2 kJ mol^{-1} respectively. The T1 diagnostics for the ~~cylcloaddition~~ reactions of singlet ~~O2~~ to toluene are both 0.019. Rate constants for those reaction channels are shown in Table 4. Even though the rate constants for reaction with singlet O_2 is much faster than that with triplet O_2, the concentration of singlet O_2 is much lower, so singlet O_2 kinetics do not contribute significantly to the total rates.

Table 4: Rate constants in the temperature range of 500 to 2000 K for $O_2(a\,^1\Delta_g)$ reactions, $k = AT^n \exp(-E_A/RT)$; units cm^3, s, cal.

Reactant	A	n	E_A
CH_2=CHC**H**$_3$	8.38×10^0	3.11	4,571
CH_2=C(C**H**$_3$)$_2$	1.08×10^2	2.98	3,213
toluene (abstraction)	7.42×10^{-2}	3.77	12,747
toluene (addition)	3.10×10^3	2.69	6,012

In order to test the importance of the reactions of singlet O_2 with toluene and to further attempt to rationalise the experiments of Oehlschlaeger *et al.*, rate constants for the inter-conversion of singlet O_2 and triplet O_2 were included in the detailed kinetic mechanism of Zhang *et al.*[7] The appropriate rate constants and collider efficiencies for the reactions:

$$O_2(a\,^1\Delta_g) + M \rightarrow O_2(X\,^1\Sigma_g^-) + M$$

$$O_2(a\,^1\Delta_g) + \dot{H} \rightarrow O_2(X\,^1\Sigma_g^-) + \dot{H}$$

$$O_2(a\,^1\Delta_g) + \ddot{O} \rightarrow O_2(X\,^1\Sigma_g^-) + \ddot{O}$$

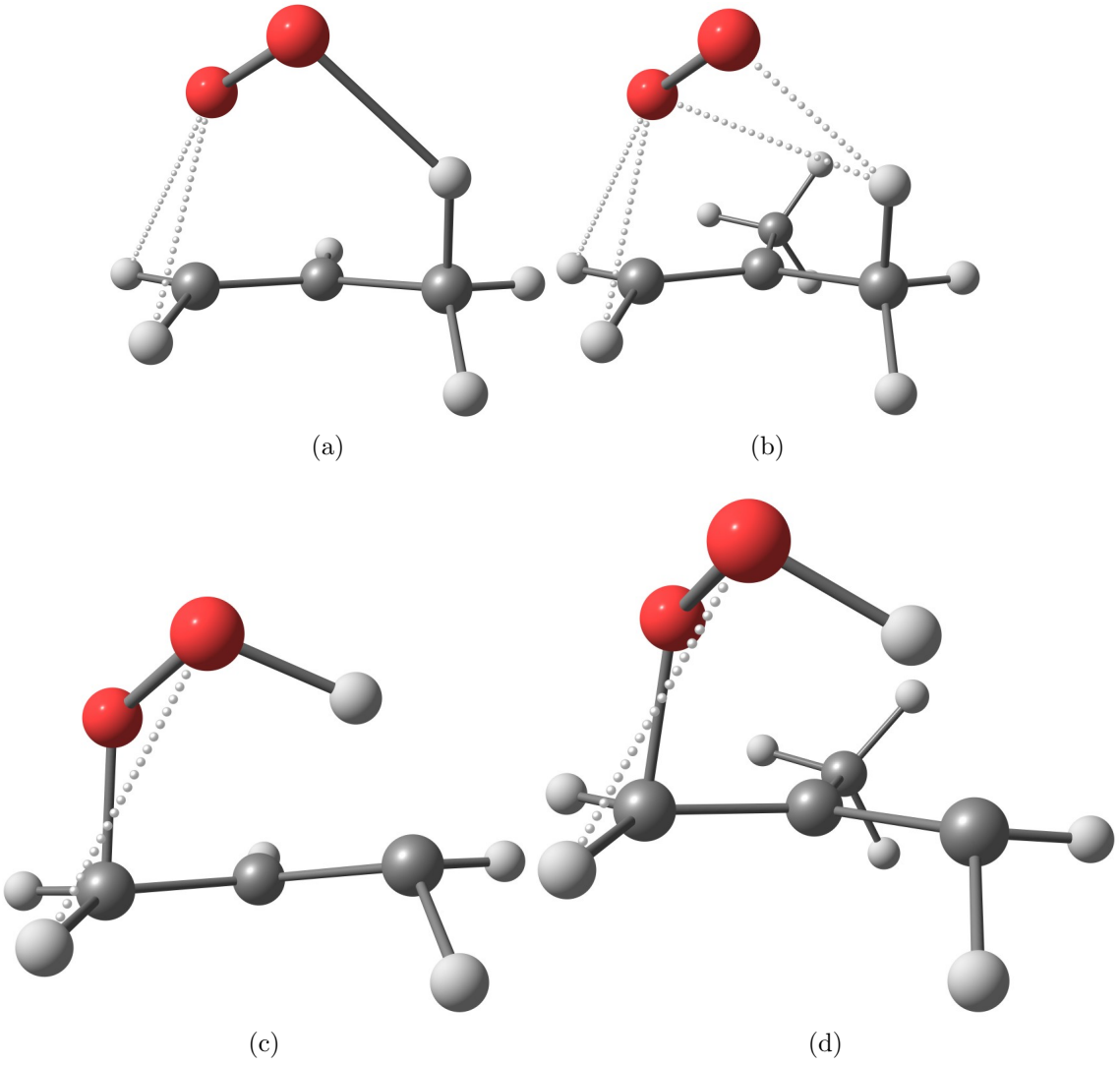

(a) (b)

(c) (d)

Figure 6: Transition states and products geometres for propene, isobutene react with singlet O_2.

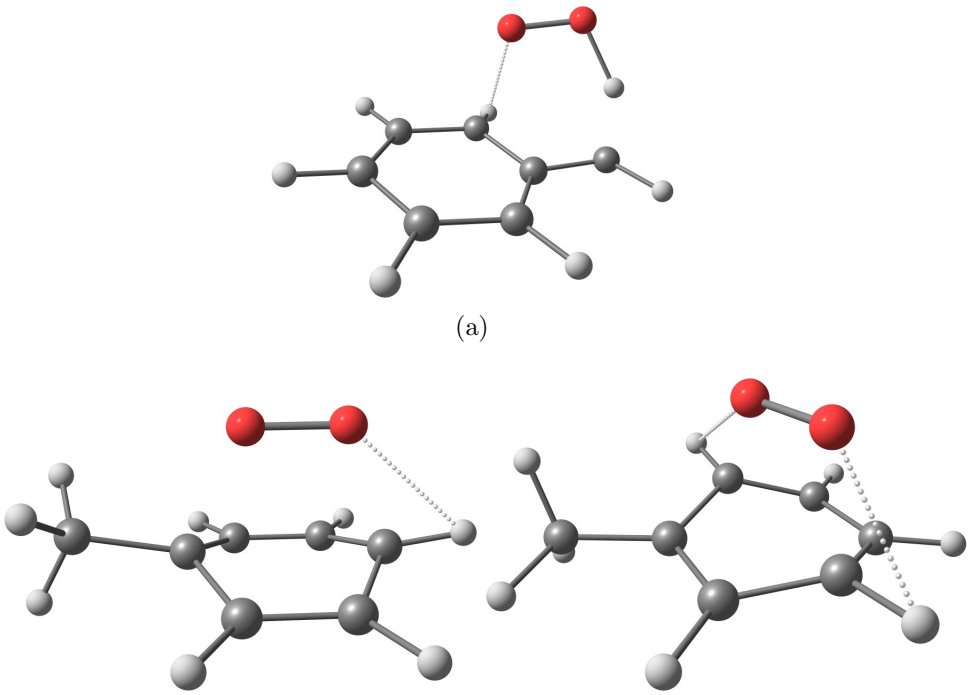

(a)

(b) (c)

Figure 7: Transition states for toluene reacts with singlet O_2 through hydrogen abstraction and addition reactions.

$$O_2(a\,^1\Delta_g) + \ddot{O} + M \rightarrow O_2(X\,^1\Sigma_g^-) + \ddot{O} + M$$

were incorporated into the kinetic model based on a scheme derived by Konnov.[47] Thermochemistry for singlet O_2 was computed herein *via* the Thermo module of Multiwell and was also included in the kinetic model, along with rate constants for the abstraction and addition reactions of singlet O_2 with toluene, as reported in Table 4. The results were quite unremarkable in that the predicted yields of toluene, benzyl and $O_2(X\,^1\Sigma_g^-)$ were completely unchanged, and so one must conclude that reactions of singlet O_2 with toluene are not important under the conditions of the Oehlschlaeger *et al.* experiments.

Rate constants summary

Apart from comparing with the available experimental results of hydrogen atom abstraction from propene, isobutene and toluene by molecular oxygen which are available in the liter-

ature, we also calculated a series of molecules with primary, secondary, tertiary and super secondary allylic hydrogen atoms of alkenes, furans and alkyl-benzene family in this work. Those molecules include 2-butene and 2-methylfuran containing the primary allylic hydrogen atom; 1-butene, 1-pentene, 2-ethylfuran, ethylbenzene and n-propylbenzene containing the secondary allylic hydrogen atom; 3-methyl-1-butene, 2-isopropylfuran and isopropylbenzene containing tertiary allylic hydrogen atom; and 1-4-pentadiene containing super allylic secondary. Total rate constants for the allylic hydrogen atom abstraction reaction rate constants are shown in Table 5.

Table 5: Rate constants in the temperature range of 500 to 2000 K for hydrogen atom abstraction by $O_2(X\,^3\Sigma_g^-)$, $k = AT^n \exp(-E_A/RT)$; units cm^3, s, cal.

Reactant	A	n	E_A
Primary			
CH_2=CHC**H**$_3$	1.77×10^1	3.64	37,300
CH_2=C(C**H**$_3$)$_2$	1.03×10^3	3.19	37,900
C**H**$_3$CH=CHC**H**$_3$	7.74×10^1	3.52	36,200
2-methylfuran	9.81×10^{-1}	3.98	37,400
toluene	1.01×10^3	3.24	39,600
Secondary			
CH_2=CHC**H**$_2$CH$_3$	4.88×10^1	3.48	34,800
CH_2=CHC**H**$_2$CH$_2$CH$_3$	6.06×10^1	3.45	34,600
2-ethylfuran	1.95×10^1	3.52	35,100
ethylbenzene	4.27×10^2	3.11	37,600
n-propylbenzene	1.80×10^3	2.90	37,700
Tertiary			
CH_2=CHC**H**(CH$_3$)$_2$	6.02×10^3	3.03	32,900
2-isopropylfuran	2.98×10^3	2.75	32,500
isopropylbenzene	6.39×10^4	2.47	37,000
'Super' Secondary			
CH_2=CHC**H**$_2$CH=CH$_2$	4.82×10^{-1}	4.16	29,900

Model application

A series of simulations have been carried out to show the influence of the rate constants calculated in this work to the ignition delay time of the fuels of 1-butene,[3] 2-butene,[4] isobutene,[2]

2-methylfuran,[5] 2,5-dimethylfuran[6] and toluene,[7] as shown in Figs. 8 and 9. Generally, the new rate constants decreased the reactivity predictions of the target fuels by a factor of 1.5 to 3 and that influence changes with temperature. For the butene isomers, the new calculated rate constants increase the ignition delay time by a factor of 1.5 to 2; while for the furans and toluene, that influence is larger which can reach a factor of 2.5 to 3. Further analysis and improvement of the reactivity prediction for the target fuels detailed chemistry model is beyond the scope of this work.

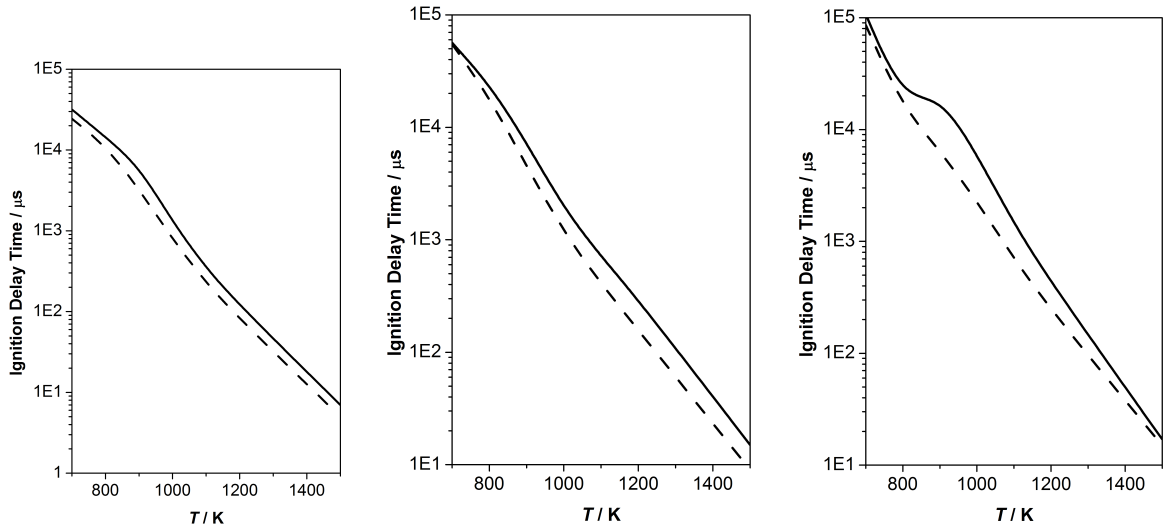

(a) (b) (c)

Figure 8: Ignition delay time predictions for (a) 1-butene, (b) 2-butene and (c) isobutene by using the rate constants calculated in this work (—) and in previous model (– – –).

Conclusion

We carried out a systematic investigation of hydrogen atom abstraction from a series of molecules with primary, secondary, tertiary and super secondary allylic hydrogen atoms by molecular oxygen. General trends have been outlined showing how the barrier to reaction changes as the nature of the hydrogen atom being abstracted goes from primary through secondary to tertiary. The effect of further methyl substitution of the propene skeleton is also

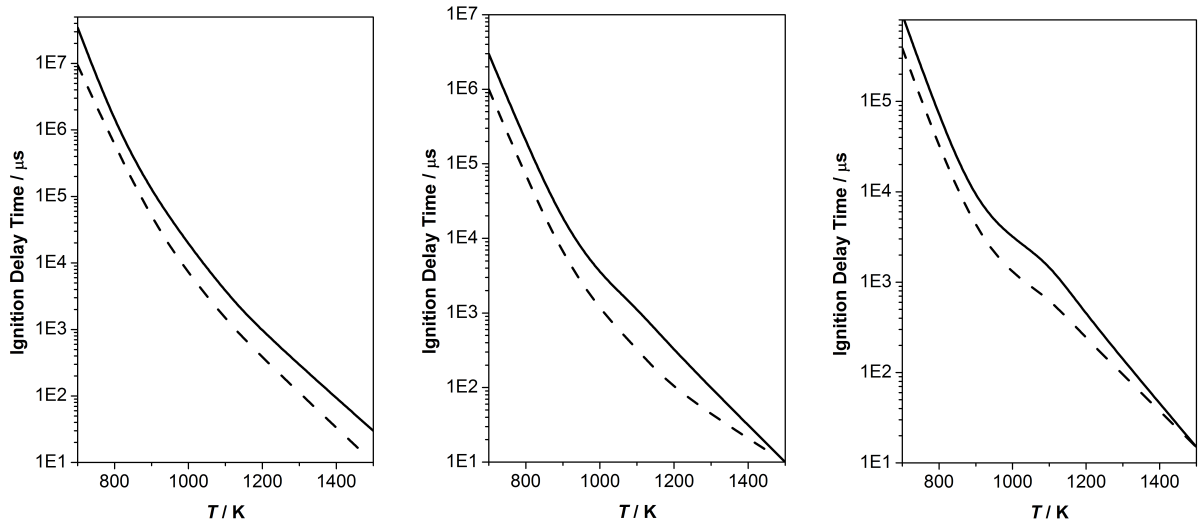

(a) (b) (c)

Figure 9: Ignition delay time predictions for (a) toluene, (b) 2-methylfuran and (c) 25-dimethylfuran by using the rate constants calculated in this work (—) and in previous model (– – –).

discussed. The concern *here* is to show the trends as the reactants are altered; some species will show more complex reactivity than straightforward H-atom abstraction. This is evident in the recent G4MP2 work by Song et al. on the reaction of thiophene and 2-methylthiophene with both singlet and triplet molecular oxygen.[48]

Numerically, our computed rate constants are in only moderate accord with the only available measurements. In two cases, propene and isobutene, our calculated rate constants are *lower* than experiment which given the potential sources of error in determining kinetic parameters in batch reactors is encouraging. Note that in relative terms however our calculations show that isobutene is 4× more reactive than propene at temperatures near $\sim$ 700 K which is in very good agreement with the Walker experiments.[10,13] The rate constants for toluene with O_2 are about an order magnitude slower than the experimentally derived rate constants from a comprehensive model proposed by Oehlschlaeger and co-authors.[15] The results clearly indicate the need for a more detailed investigation of the combustion kinetics of toluene oxidation and its key pyrolysis and oxidation intermediates. Despite this, our

computed barriers and rate constants retain an important internal consistency. This work provides a first systematic study on those key initiation reactions for compounds containing allylic hydrogen atoms.

Acknowledgement

We appreciate the support from Saudi Aramco under the FUELCOM program. The Irish Centre for High-End Computing, ICHEC, is thanked for the provision of computational resources. C. F. Goldsmith gratefully acknowledges financial support from Brown University.

References

(1) Burke, S. M.; Metcalfe, W.; Herbinet, O.; Battin-Leclerc, F.; Haas, F. M.; Santner, J.; Dryer, F. L.; Curran, H. J., An experimental and modeling study of propene oxidation. Part 1: Speciation measurements in jet-stirred and flow reactors. Combust. Flame 2014, 161 (11), 2765-2784.

(2) Zhou, C.-W.; Li, Y.; O'Connor, E.; Somers, K. P.; Thion, S.; Keesee, C.; Mathieu, O.; Petersen, E. L.; DeVerter, T. A.; Oehlschlaeger, M. A.; Kukkadapu, G.; Sung, C.-J.; Alrefae, M.; Khaled, F.; Farooq, A.; Dirrenberger, P.; Glaude, P.-A.; Battin-Leclerc, F.; Santner, J.; Ju, Y.; Held, T.; Haas, F. M.; Dryer, F. L.; Curran, H. J., A comprehensive experimental and modeling study of isobutene oxidation. Combust. Flame 2016, 167, 353-379

(3) Li, Y.; Zhou, C.-W.; ; Curran, H. J., A comprehensive experimental and modelling study of 1-butene oxidation. Submitted.

(4) Li, Y.; Zhou, C.-W.; Somers, K. P.; Zhang, K.; Curran, H. J., The oxidation of 2-butene: A high pressure ignition delay, kinetic modeling study and reactivity comparison with isobutene and 1-butene. Proc. Combust. Inst. doi:10.1016/j.proci.2016.05.052.

(5) Somers, K. P.; Simmie, J. M.; Gillespie, F.; Burke, U.; Connolly, J.; Metcalfe, W. K.; Battin-Leclerc, F.; Dirrenberger, P.; Herbinet, O.; Glaude, P. A.; Curran, H. J., A high temperature and atmospheric pressure experimental and detailed chemical kinetic modelling study of 2-methyl furan oxidation. Proc. Combust. Inst. 2013, 34 (1), 225-232

(6) Somers, K. P.; Simmie, J. M.; Gillespie, F.; Conroy, C.; Black, G.; Metcalfe, W. K.; Battin-Leclerc, F.; Dirrenberger, P.; Herbinet, O.; Glaude, P.-A.; Dagaut, P.; Togb, C.; Yasunaga, K.; Fernandes, R. X.; Lee, C.; Tripathi, R.; Curran, H. J., A comprehensive experimental and detailed chemical kinetic modelling study of 2,5-dimethylfuran pyrolysis and oxidation. Combust. Flame 2013, 160 (11), 2291-2318.

(7) Zhang, Y.; Somers, K.P.; Mehl, M.; Pitz, W.J.; Cracknell, R.F.; Curran, H.J. Probing the antagonistic effect of toluene as a component in surrogate fuel models at low temperatures and high pressures. A case study of toluene/dimethyl ether mixtures,Proc. Combust. Inst. doi:10.1016/j.proci.2016.06.190.

(8) Park, K.; West, A.; Raheja, E.; Sellner, B.; Lischka, H.; Windus, T. L.; Hase, W. L., Singlet and triplet potential surfaces for the O-2+C2H4 reaction. J. Chem. Phys. 2010, 133 (18), 13.

(9) Manion, J. A.; Huie, R. E.; Levin, R. D.; Burgess Jr., D. R.; Orkin, V. L.; Tsang, W.; McGivern, W. S.; Hudgens, J. W.; Knyazev, V. D.; Atkinson, D. B.; Chai, E.; Tereza, A. M.; Lin, C.-Y.; Allison, T. C.; Mallard, W. G.; Westley, F.; Herron, J. T.; Hampson, R. F.;Frizzell, D. H. NIST Chemical Kinetics Database, NIST Standard Reference Database 17, Version 7.0 (Web Version), Release 1.6.8, Data version 2015.12, National Institute of Standards and Technology, Gaithersburg, Maryland, 20899-8320. `http://kinetics.nist.gov/`

(10) Stothard, N. D.; Walker, R. W., Determination of the Arrhenius Parameters for the

Initiation Reaction $C_3H_6 + O_2 \rightarrow CH_2CHCH_2 + HO_2$. J. Chem. Soc.-Faraday Trans. 1991, 87, 241–247.

(11) Barbe, P.; Baronnet, F.; Martin, R.; Perrin, D. Kinetics and modeling of the thermal reaction of propene at 800 K. Part III. Propene in the presence of small amounts of oxygen. Int. J. Chem. Kinet. 1998, 30, 503–522.

(12) Baulch, D.L.; Cobos, C.J.; Cox, R.A.; Frank, P.; Hayman, G.; Just, Th.; Kerr, J.A.; Murrells, T.; Pilling, M.J.; Troe, J.; Walker, R.W.; Warnatz, J. Evaluated kinetic data for combustion modelling. Supplement I. J. Phys. Chem. Ref. Data 1994, 23, 847–1033.

(13) Ingham, T.; Walker, R.W.; Woolford, R.E. Kinetic Parameters for the Initiation Reaction $RH + O_2 \rightarrow R + HO_2$. Proc. Combust. Inst. 1994, 25, 767–774.

(14) Eng, ,R.A.; Fittschen, C.; Gebert, A.; Hibomvschi, P.; Hippler, H.; Unterreiner, A.N.; Kinetic Investigation of the Reactions of Toluene and of p-Xylene with Molecular Oxygen between 1050 and 1400 K. Symp. Int. Combust. Proc. 1998, 27, 211–218.

(15) Oehlschlaeger, M. A.; Davidson, D.F.; Hanson, R.K. Investigation of the Reaction of Toluene with Molecular Oxygen in Shock-heated Gases, Combust. Flame 2006, 147, 195–208.

(16) Curtiss, L. A.; Redfern, P. C.; Raghavachari, K., Gaussian-4 Theory. J. Chem. Phys. 2007, 126, 084108.

(17) Gaussian 09, Revision E.01, Frisch, M. J.; Trucks, G. W.; Schlegel, H. B.; Scuseria, G. E.; Robb, M. A.; Cheeseman, J. R.; Scalmani, G.; Barone, V.; Mennucci, B.; Petersson, G. A.; et al. Gaussian, Inc., Wallingford CT, 2009.

(18) Barnes, E. C.; Petersson, G. A.; Montgomery, J. A.; Frisch, M. J.; Martin, J. M. L. Unrestricted Coupled Cluster and Brueckner Doubles Variations of W1 Theory. J. Chem. Theory Comput. 2009, 5 (10), 2687–2693.

(19) Lee, T. J.; Taylor, P. R., A Diagnostic for Determining the Quality of Single-Reference Electron Correlation Methods. *Int. J. Quantum Chem.* **1989**, 199–207.

(20) Lee, T. J., Comparison of the T_1 and D_1 Diagnostics for Electronic Structure Theory: A New Definition for the Open-Shell D_1 Diagnostic. *Chem. Phys. Letts.* **2003**, *372* (3-4), 362–367.

(21) Fukui, K., The Path of Chemical Reactions — the IRC Approach. Acc. Chem. Res. 1981, 14 (12), 363 -368.

(22) Hratchian, H. P.; Schlegel, H. B., Using Hessian Updating to Increase the Efficiency of a Hessian Based Predictor-Corrector Reaction Path Following Method. J. Chem. Theory Comput. 2005, 1 (1), 61–69.

(23) Barker, J. R.; Nguyen, T. L.; Stanton, J. F.; Aieta, C.; Ceotto, M.; Gabas, F.; Kumar, T. J. D.; Li, C. G. L.; Lohr, L. L.; Maranzana, A.; Ortiz, N. F.; Preses, J. M.; Simmie, J. M.; Stimac, P. J. MultiWell-2016 Software Suite; Barker, J. R. University of Michigan, Ann Arbor, Michigan, USA, 2016; `http://clasp-research.engin.umich.edu/multiwell/`; Barker, J. R. Multiple-well, Multiple-path Unimolecular Reaction Systems. I. MultiWell Computer Program Suite. Int. J. Chem. Kinet., 2001, 33, 232–45.

(24) Klippenstein, S. J.; Wagner, A. F.; Dunbar, R. C.; Wardlaw, D. M.; Robertson, S. H.; Miller, J. A. Variflex 2.02m, 2010.

(25) Peverati, R.; Truhlar, D. G., Improving the Accuracy of Hybrid Meta-GGA Density Functionals by Range Separation. Journal of Physical Chemistry Letters 2011, 2 (21), 2810-2817.

(26) Knizia, G.; Adler, T. B.; Werner, H. J., Simplified CCSD(T)-F12 methods: Theory and benchmarks. J. Chem. Phys. 2009, 130 (5).

(27) Goldsmith, C. F.; Harding, L. B.; Georgievskii, Y.; Miller, J. A.; Klippenstein, S. J., Temperature and Pressure-Dependent Rate Coefficients for the Reaction of Vinyl Radical with Molecular Oxygen. J. Phys. Chem. A 2015, 119 (28), 7766-7779.

(28) Georgievskii, Y.; Jasper, A. W.; Zador, J.; Miller, J. A.; Burke, M. P.; Goldsmith, C. F.; Klippenstein, S. J., PAPR: Predictive Automated Phenomenological Rates, v1.

(29) Zhao, Y.; Truhlar, D. G., The M06 Suite of Density Functionals for Main Group Thermochemistry, Thermochemical Kinetics, Noncovalent Interactions, Excited States, and Transition Elements: Two New Functionals and Systematic Testing of Four M06-Class Functionals and 12 Other Functionals. Theor. Chem. Accts 2008, 120 (1-3), 215–241.

(30) Personal communication from Jingjing Zheng, March 2014. Based on method described in Alecu, I. M.; Zheng, J. J.; Zhao, Y.; Truhlar, D. G., Computational Thermochemistry: Scale Factor Databases and Scale Factors for Vibrational Frequencies Obtained from Electronic Model Chemistries. J. Chem. Theory Comput. 2010, 6 (9), 2872–2887.

(31) Luo, Y.-R., Comprehensive Handbook of Chemical Bond Energies. CRC Press: Boca Raton, FL, 2007.

(32) Stothard, N. D.; Walker, R. W., Oxidation Chemistry of Propene in the Autoignition Region — Arrhenius Parameters for the Allyl + O_2 Reaction Pathways and Kinetic Data for Initiation Reactions. J. Chem. Soc.-Faraday Trans. 1992, 88, 2621–2629.

(33) Goldsmith, C. F.; Klippenstein, S. J.; Green, W. H., Theoretical Rate Coefficients for Allyl + HO_2 and Allyloxy Decomposition. Proc. Combust. Inst. 2011, 33, 273–282.

(34) Chen, C.-J.; Bozzelli, J.W. Thermochemical Property, Pathway and Kinetic Analysis on the Reactions of Allylic Isobutenyl Radical with O_2: an Elementary Reaction Mechanism for Isobutene Oxidation, J. Phys. Chem. A 2000, 104, 9715–9732.

(35) Bounaceur, R.; Da Costa, I.; Fournet, R.; Billaud, F.; Battin-Leclerc, F. Experimental and Modeling Study of the Oxidation of Toluene, Int. J. Chem. Kinet. 2005, 37, 25–49.

(36) Oehlschlaeger, M. A.; Davidson, D. F.; Hanson, R. K., High-temperature thermal decomposition of benzyl radicals. J. Phys. Chem. A 2006, 110 (21), 6649-6653;

(37) Oehlschlaeger, M. A.; Davidson, D. F.; Hanson, R. K., Thermal decomposition of toluene: Overall rate and branching ratio. Proc. Combust. Inst. 2007, 31, 211-219.

(38) Narayanaswamy, K.; Blanquart, G.; Pitsch, H. A consistent chemical mechanism for oxidation of substituted aromatic species, Combust. Flame 2010, 157, 1879–1898.

(39) Metcalfe, W. K.; Dooley, S.; Dryer, F. L. Comprehensive Detailed Chemical Kinetic Modeling Study of Toluene Oxidation, Energy Fuels, 2011, 25, 4915–4936.

(40) Andrae, J. C. G. Comprehensive chemical kinetic modeling of toluene reference fuels oxidation, Fuel, 2013, 107, 740–748.

(41) Yuan, W.;Li, Y.; Dagaut, P.; Yang, J.; Qi, F. Investigation on the pyrolysis and oxidation of toluene over a wide range of conditions. I. Flow reactor pyrolysis and jet stirred reactor oxidation, Combust. Flame 2015, 162, 3–21.

(42) CHEMKIN-PRO 15151, Reaction Design, San Diego, 2010.

(43) S. J. Klippenstein (Argonne National Laboratory), personal communication, August 2016.

(44) Chase, M. W., Jr., NIST-JANAF Thermochemical Tables (4th Edition), J. Phys. Chem. Ref. Data, 1998, Mono. 9, Suppl. 1.

(45) Prein, M.; Adam, W., The Schenck ene reaction: diastereoselective oxyfunctionalization with singlet oxygen in synthetic applications. Angew. Chem. Int. Ed. 1996, 35 (5), 477–494.

(46) Sebbar, N.; Bozzelli, J. W.; Bockhorn, H., Comparison of RC(=O)=OOH, RC(=O)O-OH and R(C=O)OO-H bond dissociation energies with RC-OOH, RCO-OH and RCOO-H, R as phenyl, vinyl and alkyl groups. Chem. Phys. Lett. 2015, 629, 102-112.

(47) Konnov, A.A, On the role of excited species in hydrogen combustion, Combust. Flame 2015, 162, 3755–3772.

(48) Song, X.; Fanelli, M. G.; Cook, J. M.; Bai, F.; Parish, C. A., Mechanisms for the reaction of thiophene and methylthiophene with singlet and triplet molecular oxygen. J. Phys. Chem. A 2012, 116 (20), 4934–4946.